Berberine exerts its antineoplastic effects by reversing the Warburg effect via downregulation of the Akt/mTOR/GLUT1 signaling pathway

XIAO-HONG GUO[1*], SHUI-SHAN JIANG[2*], LI-LI ZHANG[3*], JUN HU[4], DILDA EDELBEK[4], YU-QI FENG[4], ZI-XIAN YANG[4], PENG-CHAO HU[5], HUA ZHONG[6], GUO-HUA YANG[4] and FANG YANG[6]

[1]Department of Medical Biology, School of Basic Medical Sciences, Hubei University of Chinese Medicine, Wuhan, Hubei 430065; [2]Medical Security Office, Tongren Hospital of Wuhan University (Wuhan Third Hospital), Wuhan University; [3]Nursing Department, Renmin Hospital of Wuhan University, Wuhan University; [4]Department of Medical Genetics, School of Basic Medical Science, Demonstration Center for Experimental Basic Medicine Education, Wuhan University, Wuhan, Hubei 430071; [5]Department of Oncology, Xiangyang No. 1 People's Hospital, Hubei University of Medicine, Shiyan, Hubei 442000; [6]Department of Plant Sciences, College of Life Sciences, Wuhan University, Wuhan, Hubei 430072, P.R. China

Received March 22, 2021; Accepted September 1, 2021

DOI: 10.3892/or.2021.8204

Abstract. Glucose transporter 1 (GLUT1) plays a primary role in the glucose metabolism of cancer cells. However, to the best of our knowledge, there are currently no anticancer drugs that inhibit GLUT1 function. The present study aimed to investigate the antineoplastic activity of berberine (BBR), the main active ingredient in numerous Traditional Chinese medicinal herbs, on HepG2 and MCF7 cells. The results of Cell Counting Kit-8 assay, colony formation assay and flow cytometry revealed that BBR effectively inhibited the proliferation of tumor cells, and induced G_2/M cell cycle arrest and apoptosis. Notably, the results of luminescence ATP detection assay and glucose uptake assay showed that BBR also significantly inhibited ATP synthesis and markedly decreased the glucose uptake ability, which suggested that the antitumor effect of BBR may occur via reversal of the Warburg effect. In addition, the results of reverse transcription-quantitative PCR, western blotting and immunofluorescence staining indicated that BBR downregulated the protein expression levels of GLUT1, maintained the cytoplasmic internalization of GLUT1 and suppressed the Akt/mTOR signaling pathway in both HepG2 and MCF7 cell lines. Augmentation of Akt phosphorylation levels by the Akt activator, SC79, abolished the BBR-induced decrease in ATP synthesis, glucose uptake, GLUT1 expression and cell proliferation, and reversed the proapoptotic effect of BBR. These findings indicated that the antineoplastic effect of BBR may involve the reversal of the Warburg effect by downregulating the Akt/mTOR/GLUT1 signaling pathway. Furthermore, the results of the co-immunoprecipitation assay demonstrated that BBR increased the interaction between ubiquitin conjugating enzyme E2 I (Ubc9) and GLUT1, which suggested that Ubc9 may mediate the proteasomal degradation of GLUT1. On the other hand, BBR decreased the interaction between Gα-interacting protein-interacting protein at the C-terminus (GIPC) and GLUT1, which suggested that the retention of GLUT1 in the cytoplasm may be achieved by inhibiting the interaction between GLUT1 and GIPC, thereby suppressing the glucose transporter function of GLUT1. The results of the present study provided a theoretical basis for the application of the Traditional Chinese medicine component, BBR, for cancer treatment.

Correspondence to: Dr Fang Yang, Department of Plant Sciences, College of Life Sciences, Wuhan University, 299 Bayi Road, Wuchang, Wuhan, Hubei 430072, P.R. China
E-mail: fang-yang@whu.edu.cn

Dr Guo-Hua Yang, Department of Medical Genetics, School of Basic Medical Science, Demonstration Center for Experimental Basic Medicine Education, Wuhan University, 185 Donghu Road, Wuchang, Wuhan, Hubei 430071, P.R. China
E-mail: ghyang@whu.edu.cn

*Contributed equally

Key words: berberine, glucose transporter 1, antineoplastic activity, Warburg effect

Introduction

Traditional Chinese medicines, which are widely used in certain cultures and traditions worldwide, have been recommended as effective complementary and alternative medicines for numerous different types of disease by the World Health Organization (1). Berberine (BBR), which is the main active ingredient derived from Traditional Chinese medicinal herbs belonging to the *Berberidaceae*, *Ranunculaceae* and *Papaveraceae* families, has been reported to possess multiple biological and medicinal properties, including cholesterol-reducing, antioxidant, antibacterial, anti-inflammatory and immunomodulatory effects (2-4). To date, BBR has also received significant attention due to its observed therapeutic

potential in different types of cancer. Several research groups have reported that BBR exerted antineoplastic effects by inhibiting proliferation, migration and invasion, and inducing apoptosis in various cancer types, including lung (5), breast (6,7), tongue (8) and esophageal (9) cancer, as well as hepatocellular carcinoma (10), melanoma (11), glioblastoma (12) and pancreatic cancer (13). Numerous studies have also identified telomerase, DNA topoisomerase I, p53, NF-κB, Wnt/β-catenin, AMP-activated protein kinase (AMPK) and estrogen receptors as molecular targets through which BBR exerts its antitumor effects (4,8,11,12). However, although the beneficial effects of BBR appear to be partially mediated by these aforementioned targets, few studies have focused on the effects of BBR on the glucose metabolism process and associated proteins, which may represent an additional possible mechanism underlying the antineoplastic effects of BBR.

The Warburg effect is a common hallmark of cancer cells, which have an increased energy metabolic demand, but preferentially undergo glycolysis (14). Numerous studies have revealed that glycolysis levels increase in different human malignancies despite the presence of an adequate oxygen supply to support aerobic respiration (15-17). Notably, our preliminary experiments identified that BBR strongly decreased the glucose uptake ability of HepG2 and MCF7 cell lines, therefore, it was hypothesized that BBR may interfere with tumor progression by inhibiting glycolysis.

Glucose transmembrane transport is the first step of glucose metabolism and it is also the rate-limiting step of glycolysis (18). As a member of the glucose transporter family, glucose transporter 1 (GLUT1) regulates glucose transport across the cell membrane (19). Multiple studies have demonstrated that GLUT1 expression levels were upregulated and associated with a shorter overall survival in prostate, lung and pancreatic cancer (20,21). Furthermore, GLUT1 was discovered to play a key role in various types of cancer, such as hepatocellular carcinoma, and breast and renal cancer, by promoting cell proliferation, migration and invasion, and inhibiting apoptosis (22-24). However, whether GLUT1 mediates the antineoplastic effects of BBR via regulating glucose metabolism is yet to be elucidated, to the best of our knowledge.

The present study used HepG2 liver and MCF7 breast cancer cell lines, and the normal fibroblastic epithelial/myoepithelial cell line, Hs 578Bst (derived from the human breast) to investigate the biological effects of BBR. In addition, the study also determined the potential of BBR to reverse the Warburg effect and whether the underlying antineoplastic mechanism of BBR was mediated by GLUT1.

Materials and methods

Cell lines and culture. MCF7 (HTB-22), HepG2 (HB-8065) and Hs 578Bst (HTB-125) cell lines were purchased from the American Type Culture Collection and cultured routinely at 37˚C in a humidified 5% CO_2 atmosphere in DMEM containing 10% fetal bovine serum (FBS), 100 U/ml penicillin and 100 mg/ml streptomycin. All constituents used were purchased from Sigma-Aldrich; Merck KGaA.

Cell Counting Kit-8 (CCK-8) assay. The antiproliferative effect of BBR was determined using CCK-8 reagent (GLPBIO Technology, Inc.) according to the manufacturer's protocol. Briefly, cells were seeded into 96-well plates at a density of $5x10^3$ cells/well in DMEM supplemented with 10% FBS, and allowed to adhere for 24 h. Following the incubation, the cells were cultured in medium supplemented with 1% FBS in the presence or absence of different concentrations of BBR (10, 25, 50, 75 or 100 μM) (Sigma-Aldrich; Merck KGaA) for a further 24 or 48 h. The negative control group was treated with DMSO and the positive control was exposed to glucose deprivation. After the treatment, 10 μl CCK-8 reagent was added into each well and incubated at 37˚C for another 3 h. The optical densities were measured at wavelengths of 450 and 630 nm using a microplate reader (Multiskan Mk3; Thermo Fisher Scientific, Inc.).

Colony formation assay. A total of $3x10^2$ cells/well were plated into 6-well plates and cultured for 2 days. Following the initial culture, cells were treated with BBR (50 μM for HepG2 and Hs 578Bst cells; and 25 μM for MCF7 cells). Following 14 days of incubation, the cells were fixed with 4% paraformaldehyde and stained with 5% Giemsa solution (Beijing Leagene Biotech Co., Ltd.) at room temperature (RT) for 15 min. After removing the staining solution, the cells were thoroughly washed in distilled water three times and air-dried. Only the clones with >10 cells were counted under x40-magnified visual fields with an inverted light microscope (IX71; Olympus Corporation), and images of the 6-well plate were captured with a Nikon DX digital camera (D5000; Nikon Corporation).

Flow cytometric analysis of the cell cycle and apoptosis. For the cell cycle analysis, cells were seeded into a 6-well plate at a density of $1x10^6$ cells/well and incubated with BBR at 37˚C for 24 h. The cells were then trypsinized and harvested by centrifugation (200 x g) at RT for 10 min, washed with cold PBS and fixed with 70% ethanol at 4˚C overnight. Following the incubation, cells were resuspended and incubated with 50 μg/ml RNase A for 30 min at RT. After centrifugation (200 x g), the cells were resuspended in PBS and intracellular DNA was labeled with 50 μg/ml PI (Invitrogen; Thermo Fisher Scientific, Inc.) by incubation in the dark for 15 min at RT. Cell cycle analysis was performed using a flow cytometer (FACScan; BD Biosciences).

Annexin V/PI double staining was performed for apoptosis analysis. Briefly, after treatment with BBR for 24 h, $1x10^6$ cells were trypsinized, washed with cold PBS and resuspended in 200 μl binding buffer. The cells were subsequently stained with 0.5 μg/ml Annexin V-FITC and 50 μg/ml PI in the dark for 15 min, then analyzed using a FACScan flow cytometer. The apoptotic rate was calculated as the sum of the cell proportion undergoing early apoptosis (lower right quadrant) and the cell proportion undergoing late-stage apoptosis (upper right quadrant), and then the differences in the cell apoptotic rate between the BBR and control groups were compared.

The cell cycle and apoptosis data were analysed using FlowJo V10 software (Tree Star, Inc.).

Luminescence ATP detection assay. ATP levels were determined using an ATPlite Luminescence ATP assay kit (cat. no. 6016736; PerkinElmer, Inc.) according to the

manufacturer's protocol. In total, $5x10^3$ cells/well were plated into white opaque 96-well CulturPlates (PerkinElmer, Inc.) and after 24 h of incubation at 37˚C, ATP levels were determined. Briefly, 50 μl mammalian cell lysis solution (provided in the kit) was added to each well of the microplate and the plates were mixed on an orbital shaker (100 x g) for 5 min at RT to lyse the cells and stabilize the ATP. Then, 50 μl Luciferase/Luciferin substrate solution was added to each well of the microplate and mixed on the orbital shaker for 5 min. The plate was subsequently incubated in the dark for 10 min and the luminescence of each well was measured using a spectrophotometric microplate reader (EnVision™; PerkinElmer, Inc.).

Glucose uptake assay. The cell medium was harvested after BBR treatment (50 μM for HepG2 cells and 25 μM for MCF7 cells) for 24 h, and the concentration of glucose in the media was measured using a Glucose Uptake Colorimetric assay kit (cat. no. K676-100; BioVision, Inc.) according to the manufacturer's protocol. The optical density was measured at a wavelength of 412 nm using a microplate reader (Infinite F50; Tecan Group, Ltd.).

Immunofluorescence staining of GLUT1. In total, $6x10^4$ cells were plated onto glass coverslips. Following treatment with BBR (50 μM for HepG2 cells and 25 μM for MCF7 cells) for 24 h, the cells were washed three times with PBS, then fixed with 4% paraformaldehyde and permeabilizated with 0.1% Triton X-100 at RT. Non-specific binding was blocked by incubation with 5% BSA (Beijing Solarbio Science & Technology Co., Ltd.) for 30 min at RT and the cells were subsequently incubated with an anti-rabbit polyclonal GLUT1 antibody (1:1,000; cat. no. 21829-1-AP; ProteinTech Group, Ltd.) overnight at 4˚C. Following the primary antibody incubation, the cells were incubated with an Alexa Fluor 488-conjugated secondary antibody (1:200; product code ab150077; Abcam) at 37˚C for 1 h. Nuclei were stained with 10 μM Hoechst 33258 (ADooQ Bioscience) for 1 min. Stained cells were visualized using an inverted fluorescence microscope (IX71; Olympus Corporation).

Reverse transcription-quantitative PCR (RT-qPCR). Total RNA was extracted from cells using TRIzol® reagent (Takara Bio, Inc.). Total RNA (2 μg) was reverse transcribed into cDNA using a RevertAid First Strand cDNA Synthesis kit (Thermo Fisher Scientific, Inc.) for 15 min at 30˚C, 42˚C for 60 min and 72˚C for 10 min using a 10 μl reaction volume. qPCR was subsequently performed using SYBR Premix Ex Taq (Takara Bio, Inc.) according to the manufacturer's protocol, on a 7500 Real-Time PCR Detection system (Applied Biosystems; Thermo Fisher Scientific, Inc.). The qPCR reaction mixture (20 μl volume) was measured in duplicate using the following thermocycling conditions: Initial denaturation for 3 min at 95˚C, followed by 45 cycles at 95˚C for 15 sec, 60˚C for 30 sec and 72˚C for 15 min. The following primer sequences were used for the qPCR: GLUT1 forward, 5'-TGGCATCAACGCTGTCTTCT-3' and reverse, 5'-CTAGCGCGATGGTCATGAGT-3'; and β-actin forward, 5'-TGACGTGGACATCCGCAAAG-3' and reverse, 5'-CTGGAAGGTGGACAGCGAGG-3'. The mRNA relative expression levels of GLUT1 were quantified using the $2^{-\Delta\Delta Cq}$ method (25). β-actin was used as the internal reference control.

Western blotting. Cells were seeded into a 6-well plate at a density of $1x10^6$ cells/well and cultured to 70-90% confluence, and then incubated with BBR (50 μM for HepG2 cells and 25 μM for MCF7 cells) at 37˚C for 24 h. According to experimental requirements, 8 μg/ml SC79 (cat. no. SF2730; Beyotime Institute of Biotechnology), 50 μM MG-132 (cat. no. HY-13259; MedChemExpress) or 50 μM Leupeptin hemisulfate (cat. no. HY-18234A; MedChemExpress) was pretreated at 37˚C for 8 h before BBR treatment. Subsequently, total protein was extracted from cells using RIPA lysis buffer (cat. no. C1053; Applygen Technologies, Inc.) supplemented with protease inhibitor cocktail (Roche Diagnostics). The total protein concentration was determined using the bicinchoninic acid (BCA) reaction, and 20 μg/lane of protein samples were separated via 8% SDS-PAGE and transferred onto PVDF membranes, which were blocked with 5% non-fat milk at RT for 90 min. Membranes were subsequently incubated with the following primary antibodies at 4˚C overnight: Rabbit anti-GLUT1 (1:1,000), rabbit anti-phosphorylated (p)-Akt-S473 (1:1,000; cat. no. AP0140; ABclonal Biotech Co., Ltd.), rabbit anti-Akt (1:1,000; cat. no. A11016; ABclonal Biotech Co., Ltd.), rabbit anti-p-mTOR-S2448 (1:1,000; cat. no. AP0094; ABclonal Biotech Co., Ltd.), rabbit anti-mTOR (1:1,000; cat. no. 20657-1-AP; ProteinTech Group, Inc.) and rabbit anti-GAPDH (1:1,000; product no. 2118S; Cell Signaling Technology, Inc.). Following the primary antibody incubation, the membranes were washed and incubated at RT for 90 min with HRP-conjugated goat anti-rabbit secondary antibody (1:3,000; cat. no. AS014; ABclonal Biotech Co., Ltd.). Protein bands were visualized using a SuperSignal™ West Pico PLUS Chemiluminescent substrate (Thermo Fisher Scientific, Inc.) on a gel imaging system (GE Healthcare), and the band density was quantified by densitometric analysis using ImageJ V1.8.0 software (NIH).

Generation of Flag- or histidine (His)-tagged proteins. The open reading frames (ORFs) of GLUT1, ubiquitin conjugating enzyme E2 I (Ubc9) and Gα-interacting protein-interacting protein at the C-terminus (GIPC) were amplified with PrimerSTAR® Max DNA Polymerase (cat. no. R045A; Takara Bio, Inc.) using cDNA as a template. The primers are as follow: Flag-GLUT1 forward, 5'-CCCAAGCTTATGGATTACAAGGACGACGATGACAAGATGGAGCCCAGCAGCAAGAAGCTGA-3' and reverse, 5'-CCGCTCGAGTCACACTTGGGAATCAGCCCCCAGG-3'; His-Ubc9 forward, 5'-CCCAAGCTTATGCATCATCACCATCACCATATGAGTAGTTTGTGTCTACAGCGTC-3' and reverse, 5'-CCGCTCGAGCTATTTAGAGTACTGTTTAGCTTG-3'; and His-GIPC forward, 5'-CCCAAGCTTATGCATC ATCACCATCACCATATGCCGCTGGGACTGGGGCGGCGGA-3' and reverse, 5'-CCGCTCGAGCTAGTAGCGGCCGACCTTGGCGTCC-3'. The cycling conditions comprised initial 5-min polymerase activation at 95˚C, followed by 30 cycles at 95˚C for 30 sec, 57˚C for 30 sec, and 72˚C for 1 min, and ultimately 72˚C for 5 min. Following the amplification, the ORF with either the Flag- or His-tag was inserted between the *Hin*dIII and *Xho*I sites of the pcDNA3.0

plasmid (Bioeagle Biotech Company, Ltd.). The resulting constructs were sequenced to verify the insertion of the desired tags.

Co-immunoprecipitation assay. Cells were seeded into 6-well plates, cultured to 70-90% confluence and then co-transfected with 2 μg Flag-GLUT1 alongside 2 μg empty, His-Ubc9 or His-GIPC plasmid into MCF7 cells using TurboFect™ DNA transfection reagent (Thermo Fisher Scientific, Inc.) according to the manufacturer's protocol. Cells were subsequently treated with 25 μM BBR or DMSO for 48 h. Following the treatment, the cells were collected and centrifuged at 200 x g for 10 min at 4˚C, washed twice with PBS and dissolved in weak RIPA lysis buffer (Beyotime Institute of Biotechnology) supplemented with 1X EDTA-free complete protease inhibitor (Roche Diagnostics). The lysates (100 μl) were pre-cleared with 20 μl Protein A/G PLUS-Agarose beads (cat. no. sc-2003; Santa Cruz Biotechnology, Inc.) at 4˚C for 2 h. The precleared lysates were subsequently incubated with anti-Flag antibody (1:50; cat. no. 8146) or anti-His antibody (1:50; cat. no. 2365; both from Cell Signaling Technology, Inc.) at 4˚C for 4 h, then with 50 μl Protein A/G PLUS-Agarose beads at 4˚C overnight. After the incubation, the Protein A/G PLUS-Agarose beads with bound proteins were washed with pre-cooled PBS containing 1X EDTA-free complete protease inhibitor four times and boiled with 60 μl 1X protein loading buffer for 10 min at 95˚C to elute the bound proteins. The co-immunoprecipitation products were detected using western blotting and anti-Flag (1:1,000) and anti-His (1:1,000) antibodies, as described in the western blotting section.

Statistical analysis. Statistical analysis was performed using GraphPad Prism 5.0 software (GraphPad Software, Inc.) and data are presented as the mean ± SD. Statistical differences between two groups were determined using unpaired Student's t-test, while a one-way ANOVA followed by a Bonferroni's post hoc test was used for multiple groups. $P<0.05$ was considered to indicate a statistically significant difference.

Results

Antineoplastic activity of BBR on cancer cells. To determine how BBR affected the biological traits of cancer cells, HepG2 and MCF7 cells, and normal breast cells, Hs 578Bst, were treated with different concentrations of BBR (10, 25, 50, 75 or 100 μM) and cell viability was analyzed using a CCK-8 assay. The results revealed that the viability was significantly suppressed in both cancer cell lines following BBR treatment compared with the DMSO treatment group, with the greatest reduction in viability observed in MCF7 cells, in which BBR exerted a significant cytotoxic effect at concentrations >25 μM after 48 h of treatment (Fig. 1A and B). Moreover, the antiproliferative effect of BBR on the two cancer cell lines was significantly higher compared with that on Hs 578Bst cells (Fig. 1C).

As another indicator of cell proliferation, colony formation assays were performed. The results demonstrated that the colony-forming capacity was slightly inhibited in Hs 578Bst normal breast cells following BBR treatment, but significantly inhibited in both cancer cell lines. In particular, MCF7 cells were unable to form colonies following 50 μM BBR treatment (data not shown) and only small colonies formed after 25 μM BBR treatment (Fig. 1D). Therefore, follow-up experiments were performed using 50 μM BBR to treat HepG2 cells and 25 μM BBR to treat MCF7 cells; the negative control group was treated with DMSO and the positive control was exposed to glucose deprivation.

To further determine whether BBR affected cell proliferation, flow cytometry was used to analyze the cell cycle distribution of HepG2 and MCF7 cells. The results revealed that BBR effectively induced cell cycle arrest at the G_2M phase (Figs. 1E and S1).

When proliferation is blocked, cells may initiate the apoptotic program (26). Therefore, Annexin V/PI double staining was performed and the results revealed that BBR treatment reduced the percentage of live cells and increased the percentage of cells in the middle and late apoptotic stages (Fig. 1F).

These findings indicated that BBR may exert extensive and effective antitumor activity, which was demonstrated by its ability to inhibit cell proliferation and colony formation, induce cell cycle arrest and promote apoptosis.

Antineoplastic effects of BBR are associated with the reversal of the Warburg effect. To investigate whether the Warburg effect was a key modulator on the antineoplastic effects of BBR, ATP content and glucose uptake were analyzed using luminescence ATP detection and glucose uptake assays, respectively. The results revealed that both the ATP levels and glucose uptake capacity were significantly reduced in the cell lines following BBR treatment (Fig. 2A and B).

GLUT1 is a key regulatory component that mediates glucose transmembrane transport (20). To determine whether GLUT1 mediated the effects of BBR on glucose uptake, the expression and distribution of GLUT1 was detected. RT-qPCR analysis revealed that the mRNA expression levels of GLUT1 were not altered in HepG2 cells, but were upregulated in MCF7 cells following BBR treatment (Fig. 2C). However, western blot analysis revealed that GLUT1 expression levels were significantly downregulated in both cancer cell lines (Fig. 2D). Immunofluorescence analysis demonstrated that the green fluorescence intensity of GLUT1 was reduced in BBR-treated cells. In addition, GLUT1 was found to be located within the cell membrane in the control group, whereas following BBR treatment, the membrane distribution was diminished in HepG2 cells and was absent in MCF7 cells (Fig. 2E and F). It is worth noting that further to the significant membranous distribution of GLUT1 in BBR-untreated MCF7 cells, GLUT1 was also revealed to be located in the nucleus in both BBR treated and untreated cells (Fig. 2F).

These findings indicated that the antineoplastic effects of BBR may be associated with the regulation of GLUT1, causing the subsequent reversal of the Warburg effect.

BBR-induced reversal of the Warburg effect is mediated by the Akt/mTOR/GLUT1 signaling pathway. As it was revealed that BBR exerted a significant effect over ATP synthesis and glucose metabolism to inhibit cancer progression, the kinase activities of Akt and mTOR, classical signaling molecules that have roles in glucose metabolism, cell proliferation, survival

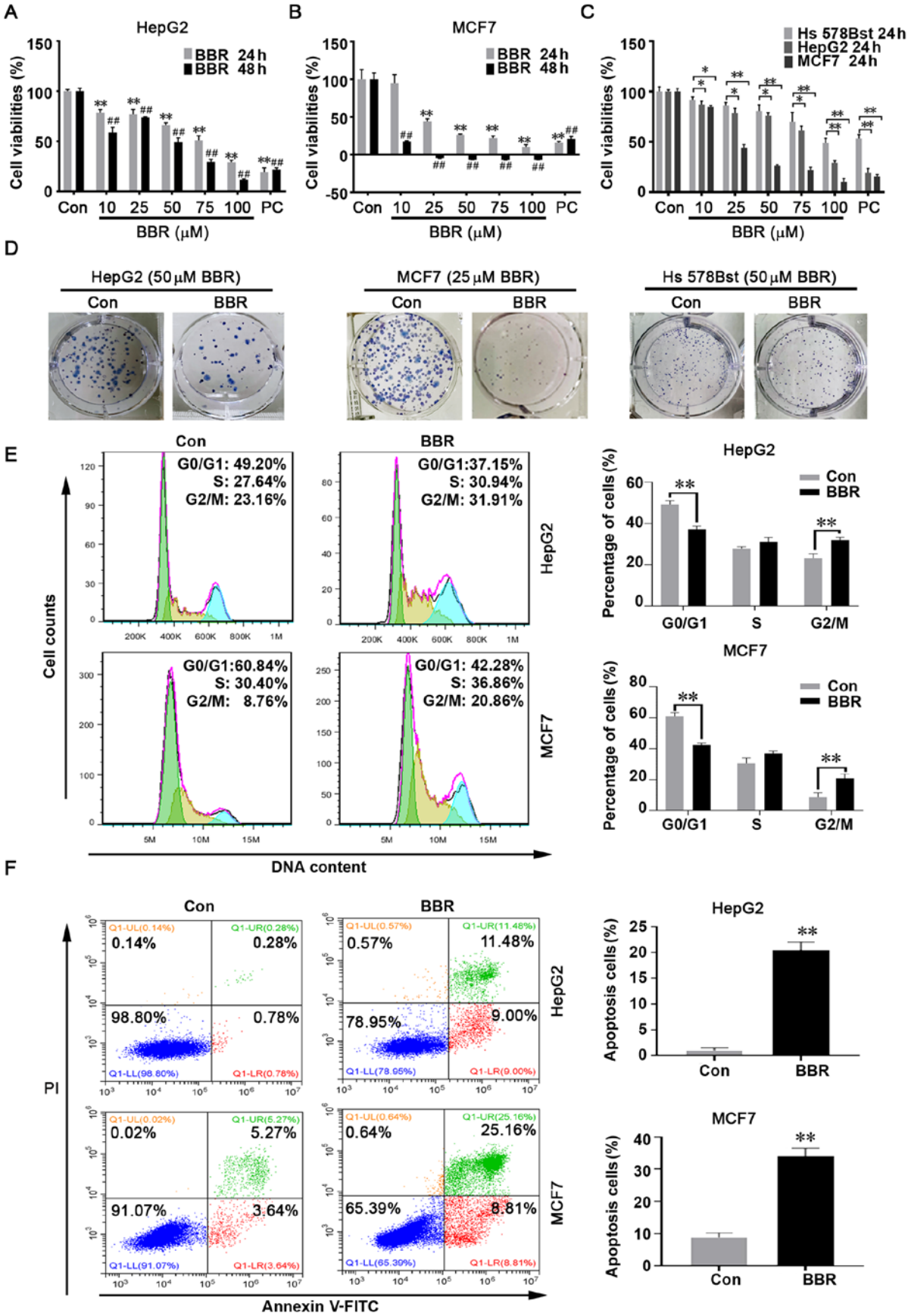

Figure 1. Antineoplastic effect of BBR on cancer cells. (A) HepG2, (B) MCF7 and (C) Hs 578Bst cells were treated with different concentrations of BBR for 24 or 48 h, and cell viability was detected using a Cell Counting Kit-8 assay. The absorbance was measured at wavelengths of 450 and 630 nm. (D) Cells were treated with 25 or 50 μM BBR for ~14 days and a colony formation assay was performed. (E) Cells were treated with BBR for 24 h, and cell cycle analysis was performed using flow cytometry. (F) Cells were incubated with BBR for 24 h and apoptosis was analyzed using Annexin V-FITC/PI double staining and flow cytometry. The flow cytometric results are presented as the percentage of cells in the different stages of apoptosis. Data are presented as the mean ± SD; n=3. *P<0.05, **P<0.01 vs. Con for 24 h and $^{\#\#}$P<0.01 vs. Con for 48 h. BBR, berberine; Con, control.

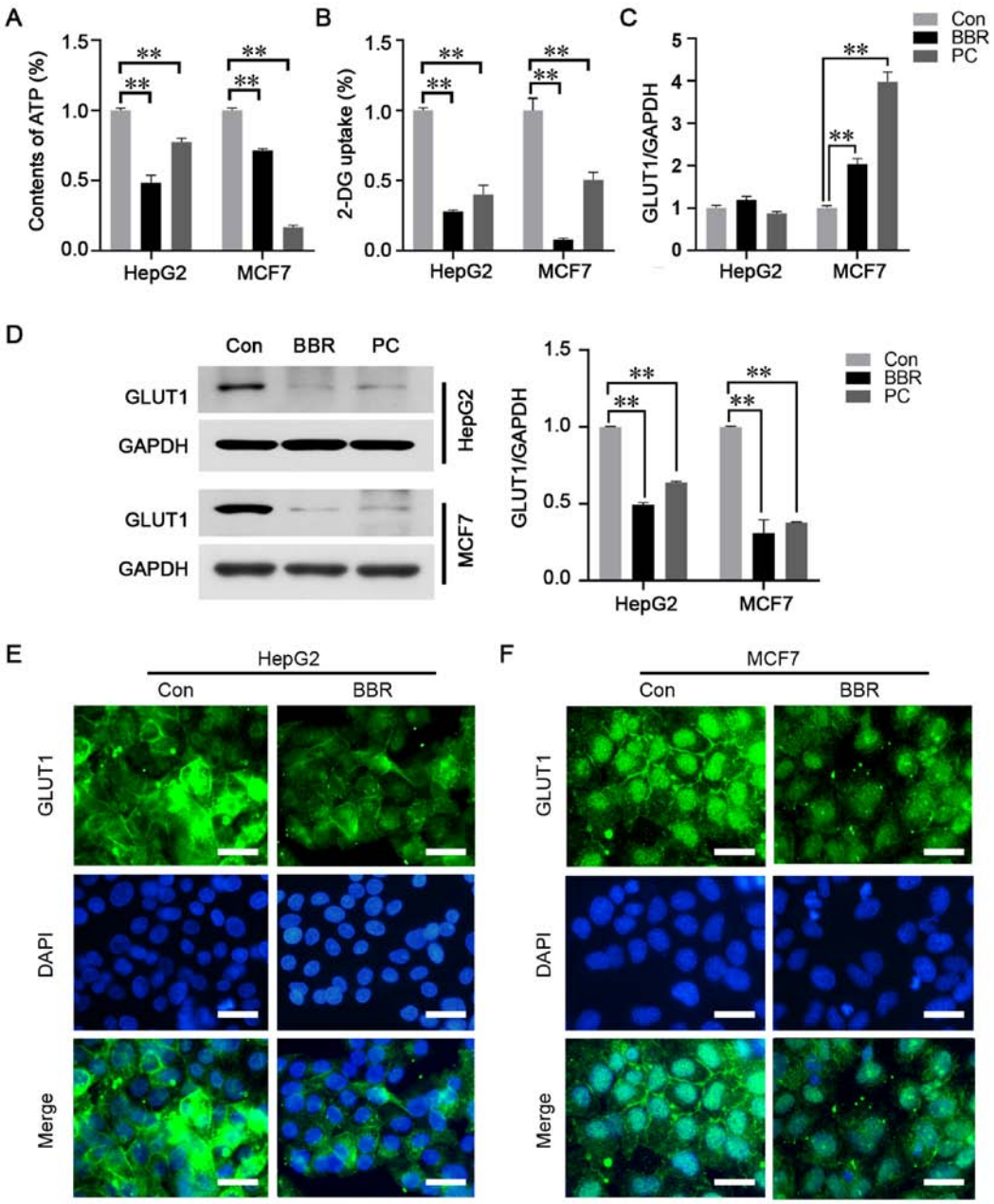

Figure 2. Antineoplastic effects of BBR are associated with the reversal of the Warburg effect. HepG2 and MCF7 cells were treated with BBR for 24 h, then the (A) content of ATP was detected using a luminescence ATP detection assay kit and (B) 2-DG uptake was detected using a glucose uptake assay kit. (C) mRNA expression levels of GLUT1 were analyzed using reverse transcription-quantitative PCR. (D) Protein expression levels of GLUT1 were analyzed using western blotting. Expression and localization of GLUT1 in (E) HepG2 and (F) MCF7 cells were determined using immunofluorescence. Scale bar, 20 μm. Data are presented as the mean ± SD; n=3. **P<0.01. BBR, berberine; GLUT1, glucose transporter 1; Con, control, PC, positive control; 2-DG, 2-deoxy-D-glucose.

and apoptosis (15), were analyzed. Western blot analysis demonstrated that the phosphorylation levels of Akt and its downstream signaling protein, mTOR, were significantly suppressed in both cancer cell lines (Fig. 3A and B). These findings suggested that BBR may exert its antineoplastic effect via regulating the Akt/mTOR signaling pathway. Cells were subsequently treated with 8 μg/ml SC79, a unique specific activator of Akt, to augment the levels of Akt phosphorylation. As anticipated, the results revealed that the BBR-induced downregulation of p-Akt, p-mTOR and GLUT1 expression levels (Fig. 3C), ATP synthesis (Fig. 3D) and glucose uptake (Fig. 3E) was abolished by SC79 pretreatment. Furthermore, the BBR-induced inhibition of viability and induction of apoptosis in HepG2 and MCF7 cells was reversed after pretreatment with SC79 (Fig. 3F-H).

These findings indicated that the BBR-induced reversal of the Warburg effect may be mediated via the Akt/mTOR/GLUT1 signaling pathway.

Downregulation of GLUT1 expression may be due to proteasomal degradation. BBR was discovered to downregulate the protein expression levels of GLUT1 and reduce the membranous distribution, which would induce GLUT1 dysfunction and prevent the transport of glucose. The most common cause of downregulated protein expression is the reduction in transcription or increase in post-translational degradation (27). As BBR

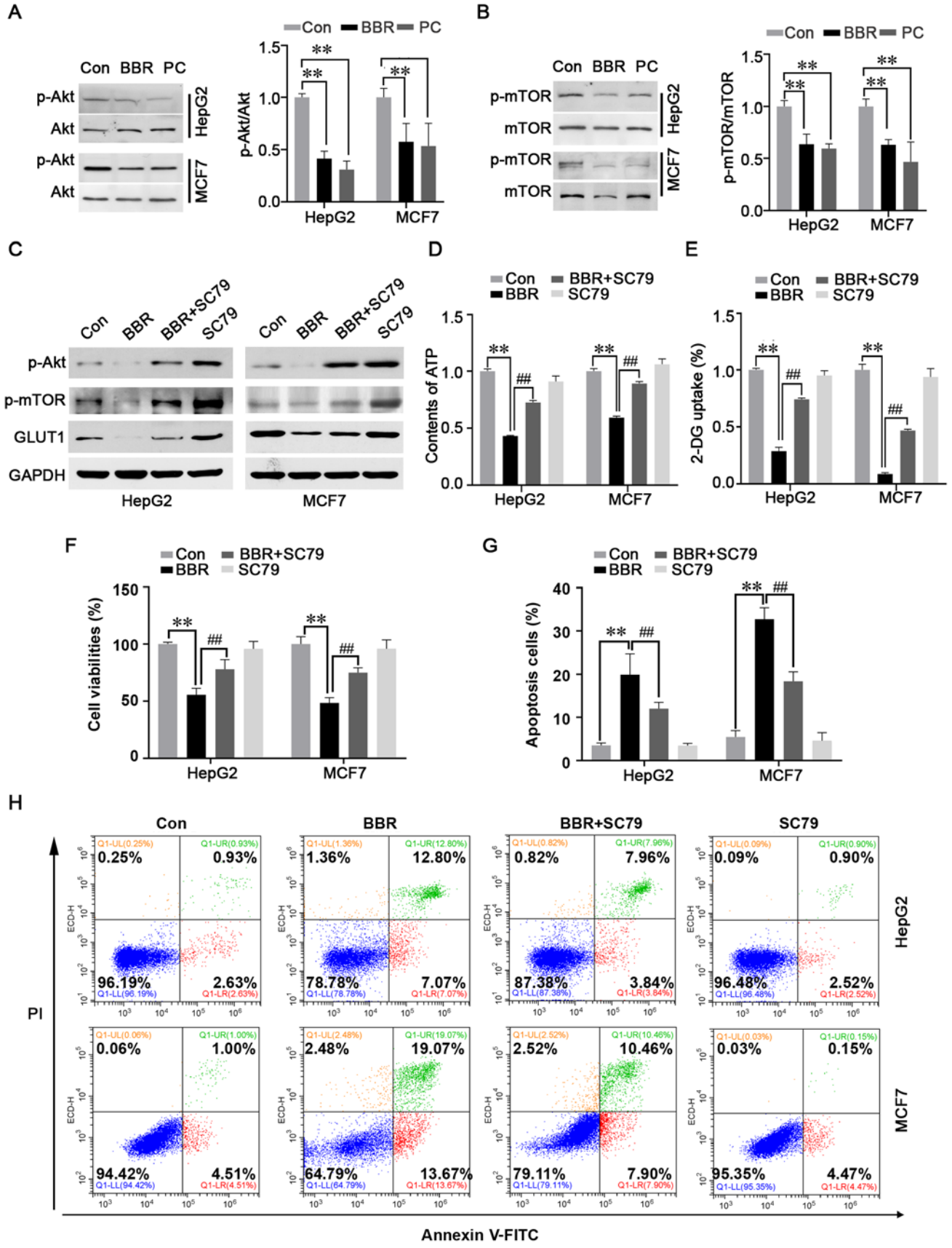

Figure 3. BBR-induced reversal of the Warburg effect is mediated by the Akt/mTOR/GLUT1 signaling pathway. Effect of BBR on the expression levels of (A) p-Akt/Akt and (B) p-mTOR/mTOR were analyzed using western blotting. Levels of phosphorylated protein were normalized to the level of corresponding total protein. Cells were pretreated with the Akt activator, SC79, prior to BBR treatment. (C) Expression levels of p-Akt, p-mTOR and GLUT1 were analyzed using western blotting. (D) ATP content was detected using a luminescence ATP detection assay kit. (E) 2-DG uptake was detected using a glucose uptake assay kit. Cells were pretreated with SC79 before BBR treatment, then the (F) viabilities of HepG2 and MCF7 cells were analyzed using a Cell Counting Kit-8 assay and the (G and H) apoptosis rate was analyzed by flow cytometry. Data are presented as the mean ± SD; n=3. **P<0.01 and $^{\#\#}$P<0.01. BBR, berberine; GLUT1, glucose transporter 1; p-, phosphorylated; 2-DG, 2-deoxy-D-glucose; Con, control; PC, positive control.

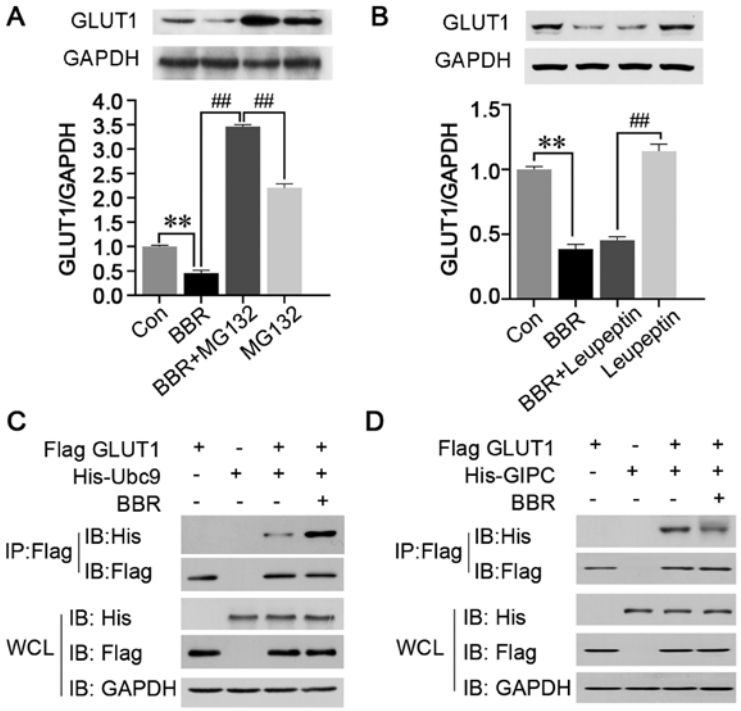

Figure 4. Ubc9 and GIPC mediate the post-translational modification and cytoplasmic retention of GLUT1, respectively. MCF7 cells were pretreated with the (A) proteasome inhibitor MG-132 or (B) lysosomal inhibitor, leupeptin, and the expression levels of GLUT1 were analyzed using western blotting. Flag-tagged GLUT1, His-tagged Ubc9 and His-tagged GIPC were constructed, and the interactions between (C) Ubc9 and GLUT1 and (D) GIPC and GLUT1 were analyzed using co-immunoprecipitation. Data are presented as the mean ± SD; n=3. **P<0.01 and $^{\#\#}$P<0.01. Ubc9, ubiquitin conjugating enzyme E2 I; GIPC, Gα-interacting protein-interacting protein at the C-terminus; GLUT1, glucose transporter 1; Con, control; His, histidine; WCL, whole cell lysate.

did not downregulate the mRNA expression levels of GLUT1 in both HepG2 and MCF7 cells (Fig. 2C), it was hypothesized that BBR may degrade GLUT1. To investigate this hypothesis, MCF7 cells were used, as the MCF7 cell line was more sensitive to BBR than the HepG2 cells. MCF7 cells were pretreated with the proteasome inhibitor, MG-132, or lysosomal inhibitor, leupeptin, to inhibit the proteasomal or lysosomal degradation pathways, respectively, prior to BBR treatment. The results revealed that the BBR-induced downregulation of GLUT1 expression levels was significantly inhibited by the pretreatment with MG-132, but not leupeptin (Fig. 4A and B). These findings indicated that the downregulated expression levels of GLUT1 may be due to proteasomal degradation.

Ubc9 may mediate the post-translational degradation of GLUT1. Ubc9, a structural homologue of the E2 ubiquitin-conjugating enzyme, was previously reported to be involved in the post-translational degradation of GLUT1 (28). Thus, co-immunoprecipitation assays using Flag-tagged GLUT1 and His-tagged Ubc9 were performed in MCF7 cells following BBR treatment. The results demonstrated that the interaction between GLUT1 and Ubc9 was significantly increased, which suggested that the BBR-induced post-translational degradation of GLUT1 may be regulated by the post-translational modifications mediated by Ubc9 (Fig. 4C).

Disruption of GIPC binding to GLUT1 may mediate the cytoplasmic retention of GLUT1. GIPC, a PDZ domain containing protein, was reported to specifically interact with the PDZ binding motif, DSQV, at the C-terminus of GLUT1, thereby promoting the stability of intracellular GLUT1 and assisting in its return to the cell membrane (29). Therefore, co-immunoprecipitation of Flag-tagged GLUT1 and His-tagged GIPC was performed in MCF7 cells following BBR treatment, and the results revealed that the interaction between GLUT1 and GIPC was disrupted (Fig. 4D). This finding indicated that BBR may lead to the retention of GLUT1 in the cytoplasm by inhibiting the binding between GLUT1 and GIPC.

The proposed mechanism of action for the antineoplastic effects of BBR, which suggests that BBR can reverse the Warburg effect via modulation of the Akt/mTOR/GLUT1 signaling pathway, is presented in Fig. 5.

Discussion

The search for novel antineoplastic drugs that are effective in tumors refractory to conventional therapy is crucial for the development of efficient anticancer therapies. BBR is a commonly used drug in Traditional Chinese medicine and recently, its reported antineoplastic effects have attracted significant attention. Previous studies have revealed that BBR inhibited proliferation, invasion and metastasis, and induced cell cycle arrest and apoptosis in multiple types of cancer (5-12). It has been reported that 500 μg/ml BBR could inhibit cell viability by 85 and 87% on HepG2 and MCF7 cells respectively, and after treatment with BBR at a low concentration of 56 μg/ml, the inhibitory rate was reduced to 19 and 11% on HepG2 and MCF7 cells respectively. When the concentration of BBR was 19 μg/ml, no inhibitory effect on HepG2 and MCF7 cells was observed (30). Another study also reported that high-doses of BBR (50 and 100 μM) markedly inhibited HepG2 cell survival by 41 and 36% respectively in

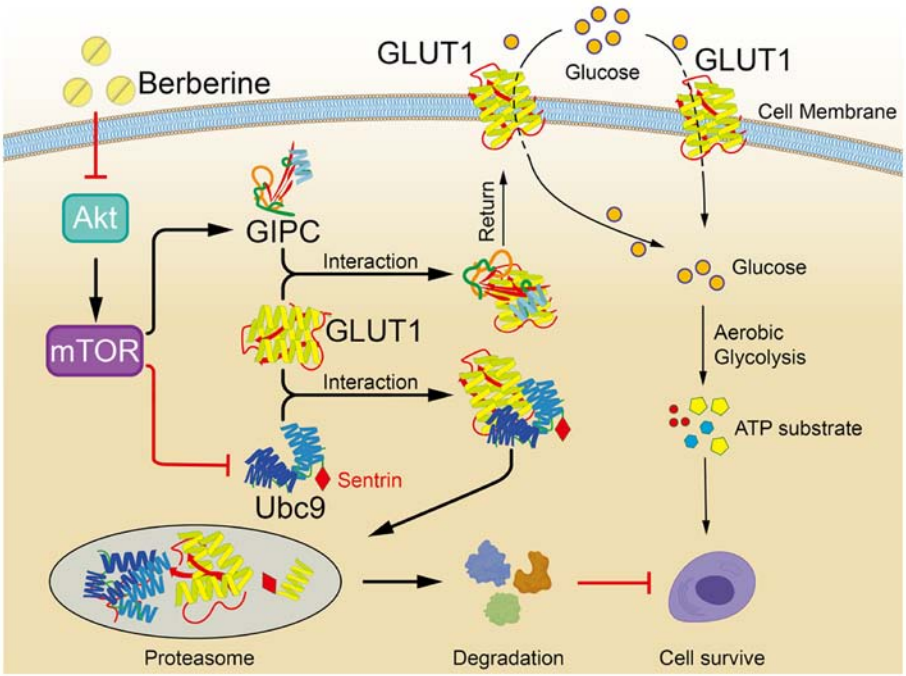

Figure 5. Proposed underlying mechanism of the antineoplastic effects of BBR, which involves the reversal of the Warburg effect via downregulating the Akt/mTOR/GLUT1 signaling pathway. Treatment with BBR downregulates the expression levels of p-Akt in cancer cells, which in turn downregulates the levels of its downstream signaling protein, p-mTOR. Subsequently, the binding between GIPC and GLUT1 is weakened, which results in the cytoplasmic retention of GLUT1. The weakened binding of GIPC with GLUT1 also strengthens the binding between Ubc9 and GLUT1, which leads to the post-translational degradation of GLUT1 and further diminishes the glucose transport function of GLUT1. Consequently, the glucose uptake capacity of cancer cells and ATP synthesis are decreased, therefore the Warburg effect of cancer cells is reversed, which contributes to the antineoplastic activity of BBR. BBR, berberine; Ubc9, ubiquitin conjugating enzyme E2 I; GIPC, Gα-interacting protein-interacting protein at the C-terminus; GLUT1, glucose transporter 1; p-, phosphorylated.

48 h, while a relative low dose of BBR (10 μM) had almost no effects on HepG2 cell survival (31). Consistent with these previous studies, the results of the present study revealed that BBR inhibited the proliferation and promoted the apoptosis of HepG2 and MCF7 cells, and also induced cell cycle arrest in the G_2M phase. Furthermore, the inhibitory rates of the concentration of BBR in cell viability in our study were approximate to or even higher than that in previous research for the same cell line (30,31). The molecular weight of BBR used in our study was 336.37 ($C_{20}H_{18}NO_4$), 10 μM was ~3.36 μg/ml, and 100 μM was ~33.6 μg/ml. In the present study, 10-100 μM BBR treatment was conducted to investigate its effect on cell viability, and was revealed to significantly suppress the cell viability in HepG2 and MCF7 cells, especially in MCF7 cells, in which BBR exerted a significant cytotoxic effect at concentrations >25 μM (8.4 μg/ml) after 48 h of treatment. Furthermore, 50 μM (16.8 μg/ml) BBR was revealed to have 34% and 51% inhibitory rates within 24 and 48 h, respectively, for HepG2 cell viability, and 74% and 107% inhibitory rates within 24 and 48 h, respectively, for MCF7 cell viability, and 25 μM (8.4 μg/ml) BBR was found to have 56 and 105% inhibitory rates within 24 and 48 h, respectively, for MCF7 cell viability. Notably, the inhibitory effects of BBR on proliferation and colony formation in the human normal breast cells, Hs 578Bst, were not as significant as the effects on the cancer cell lines used. These results indicated that BBR may represent a promising antineoplastic drug that specifically targets tumor cells, while exerting low toxicity to normal cells.

To rapidly proliferate and survive, cancer cells have a high demand for ATP, utilize glucose more rapidly and produce more lactate; however, they have a decreased demand for oxygen, which is known as the Warburg effect (32-34). It was previously reported that BBR inhibited glucose uptake and metabolism in colon cancer cells (35). Consistent with the aforementioned research (32-35), the findings of the present study demonstrated that both ATP synthesis and the glucose uptake ability were significantly decreased after BBR treatment in HepG2 and MCF7 cell lines. Furthermore, the protein expression levels of GLUT1, the main transporter involved in glucose metabolism, were also significantly downregulated, and GLUT1 was revealed to have translocated from the membrane to the cytoplasm, which suggested that the function of GLUT1 may be dysregulated in glucose metabolism. These results further indicated that BBR may target the Warburg effect and regulate glucose metabolism in cancer cells to exert its effects.

Numerous studies have attempted to determine the antineoplastic mechanisms of BBR by investigating its effects on different signaling pathways. A large number of molecular targets of BBR have been identified, including p53, NF-κB, β-catenin and AMPK (4). BBR was previously reported to suppress β-catenin signaling and cell proliferation via binding to nuclear receptor retinoid X receptor α in colon cancer (36), suppress the proliferation, migration and invasion of endometrial cancer cells via regulating the microRNA (miRNA/miR)-101/cyclooxygenase-2 axis (37) and reverse hypoxia-induced chemoresistance in breast cancer through the inhibition of the AMPK/hypoxia-inducible factor (HIF)-1α pathway (38). In addition, the combined treatment of BBR and cisplatin exerted a significant inhibitory effect

on ovarian cancer cell proliferation, arrested the cell cycle at the G_0/G_1 phase and markedly enhanced cancer cell death by inducing caspase-dependent apoptosis and receptor interacting serine/threonine kinase 3/mixed lineage kinase domain like pseudokinase-dependent necroptosis (39). It was previously revealed that BBR decreased the rate of glucose metabolism via suppression of mTOR-dependent HIF-1α protein synthesis in colon cancer cells (35). The results of the present study discovered that BBR decreased the activity of the Akt/mTOR signaling pathway in both HepG2 and MCF7 cell lines, which suggested that Akt/mTOR may be a crucial downstream mediator of the antineoplastic effects of BBR.

The Akt/mTOR signaling pathway plays important roles in numerous biological functions of cancer cells, including cell proliferation, viability, survival, glucose metabolism and protein synthesis. Its activation has been associated with cancer development and is frequently detected in malignancies (15). As important sources of anticancer molecules, numerous different natural compounds have been identified to inhibit Akt/mTOR signaling and have been associated with a reduced risk of certain cancer types. For example, in a previous study, apigenin, which is found in abundance in common fruits and vegetables, was revealed to inhibit Akt function in different cell types (40). In addition, miR-171, a miRNA found in different types of plant, was revealed to modulate the mTOR signaling pathway in 293 cells (41). In the present study, it was hypothesized that the antineoplastic activity of BBR may be due to its ability to target the Warburg effect and regulate glucose metabolism via the Akt/mTOR signaling pathway. By using a specific activator of Akt, SC79, the findings of the present study revealed that the activation of Akt diminished the inhibitory effects of BBR on ATP synthesis and glucose uptake, as well as the downregulatory effect on GLUT1 expression. Furthermore, the BBR-induced inhibition of cell viability and induction of cell apoptosis were partially abolished after pretreatment with SC79. Thus, these data indicated that the antineoplastic effects of BBR may be associated with the reversal of the Warburg effect via the downregulation of the Akt/mTOR/GLUT1 signaling pathway.

The results of the present study also demonstrated that the protein expression levels of GLUT1 were significantly downregulated in BBR-treated cancer cells, while the mRNA expression levels of GLUT1 were unaltered or in some cases, upregulated. It was hypothesized that the downregulation of GLUT1 protein expression levels may occur due to post-translational degradation. As anticipated, following the pretreatment of MCF7 cells with an inhibitor to inhibit the proteasomal degradation pathway before BBR treatment, the BBR-induced downregulation of GLUT1 expression levels was markedly abolished. In a previous study, Ubc9 was revealed to interact with GLUT1 by binding to a specific 11 amino acid sequence in the COOH terminus, and the upregulation of Ubc9 expression in L6 myoblasts decreased the cellular content of GLUT1 (28). It was suggested that Ubc9 may direct GLUT1 towards proteasome- or lysosome-mediated degradation by linking multiple residues of single sentrin (a small ubiquitin-like protein) to GLUT1 (28). In the present study, the results demonstrated that BBR promoted the interaction between Ubc9 and GLUT1 in MCF7 cells, which suggested that Ubc9 may regulate the post-translational modification of GLUT1. Concurrently, BBR also led to the retention of GLUT1 in the cytoplasm by inhibiting the binding between GLUT1 and GIPC. Therefore, it was hypothesized that the binding between GLUT1 and Ubc9 may inhibit the GIPC-mediated membrane translocation of GLUT1, resulting in the intracellular retention of GLUT1, which would suppress the glucose transporter function of GLUT1. These events would subsequently suppress the proliferation of tumor cells by inhibiting access to the energy source, glucose. The detailed mechanisms by which this mechanism may occur should be explored in future studies.

There are some limitations in the present study. Although it was demonstrated that the antineoplastic effects of BBR were associated with the reversal of the Warburg effect which was mediated by the Akt/mTOR/GLUT1 pathway *in vitro*, the effect of BBR on solid tumors still requires further validation in *in vivo* models. In addition, as one of the most used natural products worldwide, BBR is limited to poor absorption when taken orally, as well as intestinal side effects including cramping, stomach upset, and shaping gut microbiota (42). Future experiments focusing on the effects of BBR derivatives or designing BBR carriers, such as silver nanoparticles, zinc oxide nanoparticles and nanostructured lipids, should be implemented to overcome these limitations (43). In conclusion, the findings of the present study highlighted the antineoplastic activity of BBR, which was evidenced through its ability to inhibit the proliferation, induce cell cycle arrest at the G_2M phase and promote the apoptosis of cancer cells. The results of the present study also indicated that Ubc9 and GIPC may mediate the glucose transport function of GLUT1, and the antitumor effect of BBR may be attributed to its ability to reverse the Warburg effect via regulating the Akt/mTOR/GLUT1 signaling pathway. The proposed underlying mechanism of action for the antineoplastic effects of BBR is demonstrated in Fig. 5. In addition, as a well-known plant alkaloid with a long history of medicinal use in China, BBR was further demonstrated to exert low toxicity and had a high safety profile in the present study. Hence, the present results provided novel insight into the antineoplastic mechanism of BBR and suggested that BBR may represent a potential treatment strategy for cancer, highlighting the significance of Traditional Chinese medicines in cancer treatment.

Acknowledgements

Not applicable.

Funding

The present study was supported by the National Natural Science Foundation of China (grant nos. 81703015 and 31570353).

Availability of data and materials

All the datasets generated or analyzed during the present study are included in this published article.

Authors' contributions

XHG and GHY designed the study, administrated the research and were major contributors in writing the manuscript. SSJ

and LLZ performed the Cell Counting Kit-8, colony formation, flow cytometry and Co-IP experiments, analyzed the data, helped to interpret the data and revised the paper. JH, DE, YQF and ZXY participated in the experiments of ATP detection, glucose uptake assay, immunofluorescence staining and the acquisition of data. PCH and HZ cultured cells, performed RT-qPCR and western blot analysis, FY designed the study and administrated the research. PCH and FY acquired the fundings. XHG, GHY and FY confirmed the authenticity of all the raw data. All authors have read and approved the final manuscript.

Ethics approval and consent to participate

Not applicable.

Patient consent for publication

Not applicable.

Competing interests

The authors declare that they have no competing interests.

References

1. Efferth T, Xu AL and Lee DYW: Combining the wisdoms of traditional medicine with cutting-edge science and technology at the forefront of medical sciences. Phytomedicine 64: 153078, 2019.
2. Wang Y, Yi X, Ghanam K, Zhang S, Zhao T and Zhu X: Berberine decreases cholesterol levels in rats through multiple mechanisms, including inhibition of cholesterol absorption. Metabolism 63: 1167-1177, 2014.
3. Kong W, Wei J, Abidi P, Lin M, Inaba S, Li C, Wang Y, Wang Z, Si S, Pan H, *et al*: Berberine is a novel cholesterol-lowering drug working through a unique mechanism distinct from statins. Nat Med 10: 1344-1351, 2004.
4. Hou Q, He WJ, Wu YS, Hao HJ, Xie XY and Fu XB: Berberine: A Traditional Natural Product With Novel Biological Activities. Altern Ther Health Med 26S: 20-27, 2020.
5. Chen QQ, Shi JM, Ding Z, Xia Q, Zheng TS, Ren YB, Li M, and Fan LHl: Berberine induces apoptosis in non-small-cell lung cancer cells by upregulating miR-19a targeting tissue factor. Cancer Manag Res 11: 9005-9015, 2019.
6. Sun Y, Wang W and Tong Y: Berberine Inhibits Proliferative Ability of Breast Cancer Cells by Reducing Metadherin. Med Sci Monit 25: 9058-9066, 2019.
7. Refaat A, Abdelhamed S, Yagita H, Inoue H, Yokoyama S, Hayakawa Y and Saiki I: Berberine enhances tumor necrosis factor-related apoptosis-inducing ligand-mediated apoptosis in breast cancer. Oncol Lett 6: 840-844, 2013.
8. Kim JS, Oh D, Yim MJ, Park JJ, Kang KR, Cho IA, Moon SM, Oh JS, You JS, Kim CS, *et al*: Berberine induces FasL-related apoptosis through p38 activation in KB human oral cancer cells. Oncol Rep 33: 1775-1782, 2015.
9. Jiang SX, Qi B, Yao WJ, Gu CW, Wei XF, Zhao Y, Liu YZ and Zhao BS: Berberine displays antitumor activity in esophageal cancer cells in vitro. World J Gastroenterol 23: 2511-2518, 2017.
10. Luo Y, Tian G, Zhuang Z, Chen J, You N, Zhuo L, Liang B, Song Y, Zang S, Liu J, *et al*: Berberine prevents non-alcoholic steatohepatitis-derived hepatocellular carcinoma by inhibiting inflammation and angiogenesis in mice. Am J Transl Res 11: 2668-2682, 2019.
11. Kou Y, Li L, Li H, Tan Y, Li B, Wang K and Du B: Berberine suppressed epithelial mesenchymal transition through cross-talk regulation of PI3K/AKT and RARα/RARβ in melanoma cells. Biochem Biophys Res Commun 479: 290-296, 2016.
12. Maiti P, Plemmons A and Dunbar GL: Combination treatment of berberine and solid lipid curcumin particles increased cell death and inhibited PI3K/Akt/mTOR pathway of human cultured glioblastoma cells more effectively than did individual treatments. PLoS One 14: e0225660, 2019.
13. Abrams SL, Follo MY, Steelman LS, Lertpiriyapong K, Cocco L, Ratti S, Martelli AM, Candido S, Libra M, Murata RM, *et al*: Abilities of berberine and chemically modified berberines to inhibit proliferation of pancreatic cancer cells. Adv Biol Regul 71: 172-182, 2019.
14. Warburg O: On the origin of cancer cells. Science 123: 309-314, 1956.
15. Hanahan D and Weinberg RA: Hallmarks of cancer: The next generation. Cell 144: 646-674, 2011.
16. Massari F, Ciccarese C, Santoni M, Iacovelli R, Mazzucchelli R, Piva F, Scarpelli M, Berardi R, Tortora G, Lopez-Beltran A, *et al*: Metabolic phenotype of bladder cancer. Cancer Treat Rev 45: 46-57, 2016.
17. Xiao H, Wang J, Yan W, Cui Y, Chen Z, Gao X, Wen X and Chen J: GLUT1 regulates cell glycolysis and proliferation in prostate cancer. Prostate 78: 86-94, 2018.
18. Powles T, Murray I, Brock C, Oliver T and Avril N: Molecular positron emission tomography and PET/CT imaging in urological malignancies. Eur Urol 51: 1511-1520, discussion 1520-1521, 2007.
19. Deng D, Xu C, Sun P, Wu J, Yan C, Hu M and Yan N: Crystal structure of the human glucose transporter GLUT1. Nature 510: 121-125, 2014.
20. Reinicke K, Sotomayor P, Cisterna P, Delgado C, Nualart F and Godoy A: Cellular distribution of Glut-1 and Glut-5 in benign and malignant human prostate tissue. J Cell Biochem 113: 553-562, 2012.
21. Yu M, Yongzhi H, Chen S, Luo X, Lin Y, Zhou Y, Jin H, Hou B, Deng Y, Tu L, *et al*: The prognostic value of GLUT1 in cancers: A systematic review and meta-analysis. Oncotarget 8: 43356-43367, 2017.
22. Amann T, Maegdefrau U, Hartmann A, Agaimy A, Marienhagen J, Weiss TS, Stoeltzing O, Warnecke C, Schölmerich J, Oefner PJ, *et al*: GLUT1 expression is increased in hepatocellular carcinoma and promotes tumorigenesis. Am J Pathol 174: 1544-1552, 2009.
23. Oh S, Kim H, Nam K and Shin I: Glut1 promotes cell proliferation, migration and invasion by regulating epidermal growth factor receptor and integrin signaling in triple-negative breast cancer cells. BMB Rep 50: 132-137, 2017.
24. Chan DA, Sutphin PD, Nguyen P, Turcotte S, Lai EW, Banh A, Reynolds GE, Chi JT, Wu J, Solow-Cordero DE, *et al*: Targeting GLUT1 and the Warburg effect in renal cell carcinoma by chemical synthetic lethality. Sci Transl Med 3: 94ra70, 2011.
25. Livak KJ and Schmittgen TD: Analysis of relative gene expression data using real-time quantitative PCR and the 2(-Δ Δ C(T)) Method. Methods 25: 402-408, 2001.
26. Fearnhead HO, Vandenabeele P and Vanden Berghe T: How do we fit ferroptosis in the family of regulated cell death? Cell Death Differ 24: 1991-1998, 2017.
27. Boado RJ: Post-transcription modulation of the blood-brain barrier GLUT1 glucose transporter by brain-derived factors. J Neural Transm Suppl 59: 255-261, 2000.
28. Giorgino F, de Robertis O, Laviola L, Montrone C, Perrini S, McCowen KC and Smith RJ: The sentrin-conjugating enzyme mUbc9 interacts with GLUT4 and GLUT1 glucose transporters and regulates transporter levels in skeletal muscle cells. Proc Natl Acad Sci USA 97: 1125-1130, 2000.
29. Wieman HL, Horn SR, Jacobs SR, Altman BJ, Kornbluth S and Rathmell JC: An essential role for the Glut1 PDZ-binding motif in growth factor regulation of Glut1 degradation and trafficking. Biochem J 418: 345-367, 2009.
30. Balakrishna A and Kumar MH: Evaluation of Synergetic Anticancer Activity of Berberine and Curcumin on Different Models of A549, Hep-G2, MCF-7, Jurkat, and K562 Cell Lines. BioMed Res Int 2015: 354614, 2015.
31. Yu R, Zhang ZQ, Wang B, Jiang HX, Cheng L and Shen LM: Berberine-induced apoptotic and autophagic death of HepG2 cells requires AMPK activation. Cancer Cell Int 14: 49, 2014.
32. Lebelo MT, Joubert AM and Visagie MH: Warburg effect and its role in tumourigenesis. Arch Pharm Res 42: 833-847, 2019.
33. Kennedy KM and Dewhirst MW: Tumor metabolism of lactate: The influence and therapeutic potential for MCT and CD147 regulation. Future Oncol 6: 127-148, 2010.
34. Semenza GL: Tumor metabolism: Cancer cells give and take lactate. J Clin Invest 118: 3835-3837, 2008.
35. Mao L, Chen Q, Gong K, Xu X, Xie Y, Zhang W, Cao H, Hu T, Hong X and Zhan YY: Berberine decelerates glucose metabolism via suppression of mTOR dependent HIF 1α protein synthesis in colon cancer cells. Oncol Rep 39: 2436-2442, 2018.

36. Ruan H, Zhan YY, Hou J, Xu B, Chen B, Tian Y, Wu D, Zhao Y, Zhang Y, Chen X, *et al*: Berberine binds RXRα to suppress β-catenin signaling in colon cancer cells. Oncogene 36: 6906-6918, 2017.
37. Wang Y and Zhang S: Berberine suppresses growth and metastasis of endometrial cancer cells via miR-101/COX-2. Biomed Pharmacother 103: 1287-1293, 2018.
38. Pan Y, Shao D, Zhao Y, Zhang F, Zheng X, Tan Y, He K, Li J and Chen L: Berberine Reverses Hypoxia-induced Chemoresistance in Breast Cancer through the Inhibition of AMPK- HIF-1α. Int J Biol Sci 13: 794-803, 2017.
39. Liu L, Fan J, Ai G, Liu J, Luo N, Li C and Cheng Z:. Berberine in combination with cisplatin induces necroptosis and apoptosis in ovarian cancer cells. Biol Res 52: 37, 2019.
40. Tong X and Pelling JC: Targeting the PI3K/Akt/mTOR axis by apigenin for cancer prevention. Anticancer Agents Med Chem 13: 971-978, 2013.
41. Gismondi A, Nanni V, Monteleone V, Colao C, Di Marco G and Canini A: Plant miR171 modulates mTOR pathway in HEK293 cells by targeting GNA12. Mol Biol Rep 48: 435-449, 2021.
42. Alolga RN, Fan Y, Chen Z, Liu LW, Zhao YJ, Li J, Chen Y, Lai MD, Li P and Qi LW: Significant pharmacokinetic differences of berberine are attributable to variations in gut microbiota between Africans and Chinese. Sci Rep 6: 27671, 2016.
43. Farooqi AA, Qureshi MZ, Khalid S, Attar R, Martinelli C, Sabitaliyevich UY, Nurmurzayevich SB, Taverna S, Poltronieri P and Xu B: Regulation of cell signaling pathways by berberine in different cancers: Searching for missing pieces of an incomplete jig-saw puzzle for an effective cancer therapy. Cancers (Basel) 11: 478, 2019.